

Theoretical Investigations Into the Variability of the ^{15}N Solid-State NMR Parameters Within an Antimicrobial Peptide Ampullosporin A

J. CZERNEK¹, J. BRUS¹

¹Institute of Macromolecular Chemistry of the Czech Academy of Sciences, Prague, Czech Republic

Received February 26, 2018

Accepted June 28, 2018

Summary

The solid-state NMR measurements play an indispensable role in studies of interactions between biological membranes and peptaibols, which are amphipathic oligopeptides with a high abundance of α -aminobutyric acid (Aib). The solid-state NMR investigations are important in establishing the molecular models of the pore forming and antimicrobial properties of peptaibols, but rely on certain simplifications. Some of the underlying assumptions concern the parameters describing the ^{15}N NMR chemical shielding tensor (CST) of the amide nitrogens in Aib and in conventional amino acids. Here the density functional theory (DFT) based calculations were applied to the known crystal structure of one of peptaibols, Ampullosporin A, in order to explicitly describe the variation of the ^{15}N NMR parameters within its backbone. Based on the DFT computational data it was possible to verify the validity of the assumptions previously made about the differences between Aib and other amino acids in the isotropic part of the CST. Also the trends in the magnitudes and orientations of the anisotropic components of the CST, as revealed by the DFT calculations of the full periodic structure of Ampullosporin A, were thoroughly analyzed, and may be employed in future studies of peptaibols.

Key words

Antimicrobial peptides • Ampullosporin A • Amidic bond • NMR • DFT

Corresponding author

J. Czernek, Institute of Macromolecular Chemistry of the Czech Academy of Sciences, Heyrovského nám. 2, 162 06 Praha 6, Czech Republic. Fax: +420-296-809-410. E-mail: czernek@imc.cas.cz

Introduction

Antimicrobial peptides (AMPs), both naturally occurring and synthetic ones, are intensely studied as a part of the efforts aiming at the development of novel antibiotics (Bechinger 2015). Perhaps the most important group of AMPs are peptaibols (Du *et al.* 2017). Peptaibols are composed from 5 up to more than 20 amino acid residues, contain nonproteinogenic amino acids (most frequently 2-aminoisobutyric acid, Aib), their *N*-terminus is acetylated, and *C*-terminus is hydroxylated (to an amino alcohol). Typically they form helical structures, and are able to self-associate, thus forming ion-conducting pores in biological (and also in artificial) membranes (Harmouche *et al.* 2017). In the related structural investigations, the solid-state nuclear magnetic resonance (SSNMR) spectroscopy measurements are indispensable (Molugu *et al.* 2017). In particular, an important peptaibol Ampullosporin A, AmpA (Ritzau *et al.* 1997), was thoroughly studied by the SSNMR techniques. Specifically, AmpA uniformly labeled with ^{15}N was analyzed in terms of its spatial orientations by analyzing the proton-decoupled ^{15}N cross-polarization spectra, and the PISEMA (Wu *et al.* 1994) spectra which correlated the ^{15}N - ^1H dipolar coupling with the ^{15}N NMR chemical shift of the same nitrogen site (Salnikov *et al.* 2009a). However, certain simplifications had to be made about the actual NMR parameters of the respective residues of AmpA. In particular, local structural effects upon the values of these parameters were neglected. It is thus of importance that the assumption about the differences in the ^{15}N chemical shielding between Aib and classical amino acids was tested by careful

measurements carried out for two small systems, namely, *N*-Ac-Aib-OH and *N*-Ac-Leu-OH (Salnikov *et al.* 2009b).

In this work, the available X-ray diffraction (XRD) structures of AmpA (Kronen *et al.* 2003) and of closely related small compounds were employed to investigate the ^{15}N NMR chemical shielding tensors (CSTs) of the amidic nitrogens using high-level quantum chemical calculations, which are based upon the density-functional theory (DFT) and which treat the crystal as an infinite system (Charpentier 2011). The principal components of the CSTs were described in terms of their magnitudes and orientations in the crystal frame. Based on this, the isotropic part of the CST, and the angles in the reference frame of the peptide bond, were extracted and compared to the available experimental data. Owing to a very good agreement between theory and measurements, the DFT values obtained within AmpA backbone are considered to be reliable for an estimation of the residue-specific effects upon the ^{15}N NMR parameters of the amidic nitrogen sites. The variability of this ^{15}N NMR data is assessed and found to be relatively small, but non-negligible. The analyses performed here are directly applicable in the SSNMR-based investigations of other peptaibols and oligopeptides.

Methods

Structures

Ampullosporin A is a pentadecapeptide Ac-Trp¹-Ala-Aib-Aib-Leu⁵-Aib-Gln-Aib-Aib-Aib¹⁰-Gln-Leu-Aib-Gln-Leu¹⁵-ol, whose XRD structure (Kronen *et al.* 2003) also contains one acetonitrile and two water molecules. Thus, the formula unit is $\text{C}_{77}\text{H}_{127}\text{N}_{19}\text{O}_{19} \cdot \text{C}_2\text{H}_3\text{N} \cdot 2\text{H}_2\text{O}$. There is one formula unit in the asymmetric unit of the crystal, and there are only two formula units in the unit cell (508 atoms, the volume of 4.702 nm³; $P2_1$ space group). Further details can be inferred from the Cambridge Structural Database (CSD) file refcode: BEKZIP. Four related solid-phase systems were also considered here, namely, *N*-Ac-Aib-OH, *N*-Ac-Leu-OH, and tripeptides Ala-Gly-Gly $\cdot\text{H}_2\text{O}$ and Gly-Gly-Val $\cdot 2\text{H}_2\text{O}$. Their XRD structures were used. The coordinates were taken from the CSD (the Refcodes are listed in Table 1). The unit cells of these model compounds are of course much smaller than that of AmpA: they amount to 0.736, 0.982, 0.507 and 0.662 nm³ for *N*-Ac-Aib-OH, *N*-Ac-Leu-OH, Ala-Gly-Gly $\cdot\text{H}_2\text{O}$ and Gly-Gly-Val $\cdot 2\text{H}_2\text{O}$, respectively.

The five crystal structures specified above were subjected to the geometry optimization as follows. The starting geometry was taken from the corresponding XRD study, and while the unit-cell parameters were kept fixed, the internal coordinates of all the atoms were varied to minimize the crystal-lattice energy. The lattice energies were estimated using the so called van der Waals-aware Density Functional (vdW-DF) approach (Sabatini *et al.* 2012) as implemented in the QUANTUM ESPRESSO (QE) suite of codes (Giannozzi *et al.* 2009). The QE version 4.3.1 was used. The revised PBE (revPBE) functional (Hammer *et al.* 1999) was adopted, and the convergence criteria were set to (in atomic units) 1×10^{-4} and 1×10^{-5} for the total energy and for its gradient, respectively (for comparison purposes the four small systems were additionally optimized with the tighter convergence criteria accordingly amounting to 1×10^{-5} and 1×10^{-6}). The Monkhorst-Pack grids (Monkhorst *et al.* 1976) employed in the calculations of AmpA, *N*-Ac-Aib-OH, *N*-Ac-Leu-OH, Ala-Gly-Gly, and Gly-Gly-Val were accordingly $1 \times 3 \times 1$, $2 k$ -points; $3 \times 3 \times 3$, 10 ; $4 \times 2 \times 1$, 2 ; $2 \times 5 \times 3$, 9 ; and $4 \times 3 \times 2$, 8 .

NMR Parameters

Also using the 4.3.1 version of the QE program package and the revPBE-vdW-DF approach, the DFT optimized structures were subjected to the calculations of the NMR chemical shielding tensors by applying the projector augmented-wave (PAW) method (Blochl 1994). The pseudopotentials needed for the PAW-revPBE-vdW-DF computations were generated by a routine from the PSLibrary.0.3.0 version of the PSLibrary project (Dal Corso 2014). The previously established procedure (Czernek *et al.* 2013a) was employed for the comparison of the resulting eigenvalues of the ^{15}N CSTs (σ_{11} , σ_{22} , σ_{33} with $\sigma_{11} \leq \sigma_{22} \leq \sigma_{33}$), and of the isotropic ^{15}N chemical shielding (σ^{iso} ; $\sigma^{\text{iso}} = (\sigma_{11} + \sigma_{22} + \sigma_{33})/3$), with their experimental counterparts, which accordingly are the eigenvalues of the ^{15}N NMR chemical shift tensors (δ_{11} , δ_{22} , δ_{33} presented here in the order following the decrease of the corresponding chemical shielding: $\delta_{33} \geq \delta_{22} \geq \delta_{11}$), and the ^{15}N isotropic chemical shift ($\delta^{\text{iso}} = (\delta_{11} + \delta_{22} + \delta_{33})/3$). Thus, the referencing of the chemical shift (Harris 2007) was avoided by the linear fit of the chemical shift tensor data, δ_{ii} , to the appropriate chemical shielding data, σ_{jj} : $\sigma_{jj} = p \delta_{ii} + q$ (in a shorthand notation). The resulting values of the slope, p , and of the intercept, q , were then used to extract the pertinent chemical shift tensor components, ε_{ii} , from $\varepsilon_{ii} = p \sigma_{jj} + q$, to arrive at an estimate of the theoretical

chemical shift (Czernek *et al.* 2014) of given nucleus, ε^{iso} , obtained as the average of ε_{11} , ε_{22} , and ε_{33} of this nucleus: $\varepsilon^{\text{iso}} = (\varepsilon_{11} + \varepsilon_{22} + \varepsilon_{33})/3$.

The DFT structures were also used to establish the orientation in the frame of the peptide bond of the eigenvectors associated with the respective eigenvalues of the ^{15}N CSTs. Here the peptide plane was defined as in the corresponding experimental study (Wadell *et al.* 2005) by the positions of the C_α and N_{amid} atoms of the investigated amino acid and of the carbonyl carbon C_O preceding this N_{amid} . The angle α describes the projection

into the $\text{C}_\text{O}\text{N}_{\text{amid}}\text{C}_\alpha$ plane of the eigenvector ξ_1 associated with the most shielded eigenvalue, σ_{11} , of given ^{15}N CST. Further, the angle β is taken between a ξ_1 and the vector pointing in the direction of the bond between the corresponding N_{amid} and its amidic proton, H_{amid} . Finally, γ is the angle subtended between the direction of the normal to the $\text{C}_\text{O}\text{N}_{\text{amid}}\text{C}_\alpha$ plane and the eigenvector ξ_2 associated with the mid-shielded eigenvalue, σ_2 , of given ^{15}N CST. In Tables 1 and 2, the respective $\text{C}_\text{O}\text{N}_{\text{amid}}\text{C}_\alpha$ plane is referred to as ‘reference plane’, while the $\text{N}_{\text{amid}} - \text{H}_{\text{amid}}$ vector as ‘bond vector’.

Table 1. The parameters related to the ^{15}N NMR data of the amidic nitrogens of the model solid-phase systems described in the text (the PAW-revPBE-vdW-DF theoretical values are listed together with the available experimental counterparts).

Parameter		<i>N</i> -Ac-Aib-OH	<i>N</i> -Ac-Leu-OH	Gly-Gly-Val dihydrate	Ala-Gly-Gly monohydrate
<i>CSD refcode</i>		COYPUB	ACLLEU01	CUWRUH	CALXES20
<i>Bond vector</i>		N69 – H2	N93 – H15	N62 – H6	N46 – H8
<i>Reference plane</i>		C46; N69; C47	C61; N93; C64	C44; N62; C45	C33; N46; C34
α (degrees)		1	7	1 (1) ^{*1}	12 (11) ^{*1}
β (degrees)		1	17	18 (20) ^{*1}	23 (23) ^{*1}
γ (degrees)		12	8	44 (36) ^{*1}	23 (15) ^{*1}
<i>The most shielded (ppm)</i>	σ^{*3}	-46.0435	-30.8340	-20.8842	-7.6822
	ε	246.3	232.1	223	211
	δ	244.0 ^{*2}	233.5 ^{*2}	218 ^{*1}	207 ^{*1}
<i>The mid-shielded (ppm)</i>	σ^{*3}	108.0251	121.6167	149.2495	153.3148
	ε	102.7	90.1	64	61
	δ	104.0 ^{*2}	94.5 ^{*2}	63 ^{*1}	59 ^{*1}
<i>The least shielded (ppm)</i>	σ^{*3}	143.5847	155.7567	158.1071	164.0947
	ε	69.6	58.3	56	50
	δ	68.0 ^{*2}	55.0 ^{*2}	53 ^{*1}	48 ^{*1}
<i>Isotropic part (ppm)</i>	σ^{iso}	68.5	82.2	95.5	103.2
	ε^{iso}	139.5	126.8	114	107
	δ^{iso}	140.0 ^{*2}	128.0 ^{*2}	111 ^{*1}	105 ^{*1}

^{*1} Wadell *et al.* 2005, ^{*2} Salnikov *et al.* 2009b, ^{*3} unrounded value as obtained from the QE program.

Results

The calibration using small systems

The ^{15}N chemical shielding parameters of the amidic nitrogen in powder samples of *N*-Ac-Aib-OH and *N*-Ac-Leu-OH were measured in order to characterize the differences in the ^{15}N CSTs between Aib and conventional

amino acids (Salnikov *et al.* 2009b). Table 1 summarizes the experimental values together with the results of the PAW-revPBE-vdW-DF computations. In particular, the values of the theoretical counterparts to the principal elements of the two ^{15}N chemical shift tensors (six data points in total) were estimated using the fitting procedure outlined in Methods section (the resulting calibration is

$\varepsilon_{ii}=0.9316 \sigma_{jj}+203.4$ ppm, with the standard error of the slope, the standard error of the intercept, the standard deviation, and the adjusted R^2 of 0.016, 1.8 ppm, 2.9 ppm, and 0.99852, respectively). This way, the differences in ε_{33} , ε_{22} , ε_{11} between *N*-Ac-Aib-OH and *N*-Ac-Leu-OH are obtained, which accordingly amount to 14.2, 12.6, and 11.3 ppm (Table 1). These values agree well with the corresponding differences in δ_{33} , δ_{22} , δ_{11} (of 10.5, 9.5, and 13.0 ppm, respectively) considering the measurement uncertainty of ± 2 ppm (Salnikov *et al.* 2009b). In addition, the difference of the isotropic chemical shifts (12.0 ppm) is recovered using the respective ε^{iso} values, as it amounts to 12.7 ppm (Table 1).

The single-crystal (SC) ^{15}N SSNMR measurements were performed on the amidic nitrogen of the Gly2 residues in the tripeptides Ala-Gly-Gly and Gly-Gly-Val, and revealed the orientation in the crystal frame of the eigenvectors associated with the respective principal elements of the investigated CSTs (Wadell *et al.* 2005). In particular, it should be noted that the orientation of the ξ_2 may substantially differ from the direction of the normal to the peptide plane (see the values of the angle γ in Table 1). Taking into account the error of the determination of α , β , γ angles of $\pm 3^\circ$ (Wadell *et al.* 2005), the PAW-revPBE-vdW-DF results are in a good accord with measurements (Table 1). Consequently, the predictions made for the sites of AmpA are discussed in the next section. Also the level of agreement between the principal elements of the ^{15}N CSTs and of the corresponding chemical shift tensors was checked for the two tripeptides, and was found to be fairly similar to that described above for *N*-Ac-Aib-OH and *N*-Ac-Leu-OH. The calibration specified above was thus applied to all four systems to extract the ε values presented in Table 1 (an alternative parametrization based on all twelve data points would be $\varepsilon_{ii}=0.9283 \sigma_{jj}+201.7$ ppm, with the standard error of the slope, the standard error of the intercept, the standard deviation, and the adjusted R^2 of 0.0095, 1.1 ppm, 2.6 ppm, and 0.99886, respectively). Since the experimental uncertainty in the values of the principal components of the chemical shift tensors determined from the SC SSNMR experiments was ± 2 ppm (Wadell *et al.* 2005), all the ε values can be considered to be closely matching their δ counterparts (Table 1). Importantly, practically the same results were obtained for the four small systems when the tighter convergence criteria, described in Methods and in the previous work (Czernek 2015), were applied during the underlying revPBE-vdW-DF geometrical optimization.

Ampullosporin A

As many as 395 optimization cycles were required to meet the convergence criteria of the revPBE-vdW-DF geometrical optimization, which started from the solid-phase structure of AmpA (Kronen *et al.* 2003). The average gradient norm per atom of the final structure was 3.4×10^{-6} , while the maximal gradient norm at an atom (the nitrogen of acetonitrile): 8.3×10^{-6} atomic units. The geometrical optimization was run on 16 cores of a computer with Intel Xeon® processors, and took about 79 days of CPU time (followed by analogous 74 CPU h of the chemical shielding calculation). Interestingly, this lengthy process resulted in only small structural differences between the experimental and DFT optimized structures (their overlay is in Figure 1). The conformation of the backbone is unaltered, and changes in the positions of side chain atoms are marginal. However, the geometrical optimization of an XRD structure is considered to be a crucial step in obtaining highly accurate ^{15}N CST data (Czernek *et al.* 2013b, Kalakewich *et al.* 2015, Soss *et al.* 2017).

For all 15 amidic nitrogens (out of which 8 belong to Aib residues) of AmpA, the values of the parameters describing the PAW-revPBE-vdW-DF ^{15}N CSTs (their magnitudes and orientations in the peptide frame) are collected in Table 2. The specific atoms used in the extraction of α , β , γ angles are also listed in Table 2 (files with the DFT optimized geometries of all the systems studied here can be obtained from the corresponding author upon request). In Table 3, the corresponding averages (together with the value of one standard deviation wherever applicable) are summarized, both theoretical and obtained experimentally (Salnikov *et al.* 2009b). It should be noted, though, that the measured data are only averages, and slightly different values were used in spectral simulations carried out by the same group (Salnikov *et al.* 2009a). Nevertheless, the DFT results compare favorably to experiment. Specifically, the differences in δ^{iso} and ε^{iso} (see Methods) between the averages for Aib and for classical amino acid residues accordingly amount to 12 and 8.7 ppm. The predicted site-specific CSTs can thus be directly employed in the simulations of AmpA in the models of oriented samples, with the goal of describing the behavior of peptaibols in membrane environments (Nagao *et al.* 2015).

Discussion

The DFT calculations of the NMR parameters in

periodic solids can now usefully supplement spectroscopical investigations in numerous areas of chemistry and materials science (Bonhomme *et al.* 2011). Here their accuracy was checked in the description of the ^{15}N chemical shielding of amidic nitrogens of Aib and classical amino acid sites in four small systems. An inspection of Table 1 shows that the trends in measured data, of both the magnitudes and the

orientations of ^{15}N CSTs, were quantitatively reproduced. Moreover, employing the calibration which included only *N*-Ac-Aib-OH and *N*-Ac-Leu-OH data, it was possible to obtain fairly accurate estimates also for the investigated glycines of Ala-Gly-Gly and Gly-Gly-Val tripeptides. It is thus assumed that the results computed analogously for the 15 sites of AmpA are fully reliable.

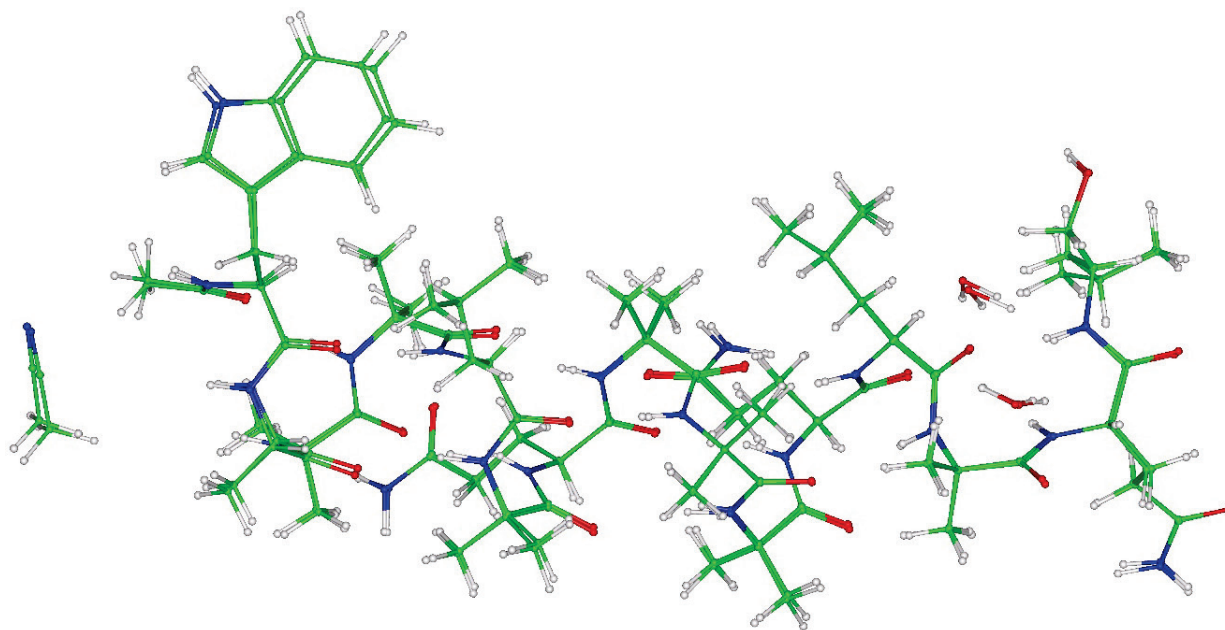


Fig. 1. The best fit of the coordinates of the experimental and DFT optimized structures of Ampullosporin A (together with crystal acetonitrile and water molecules).

Table 2. The site-specific PAW-revPBE-vdW-DF theoretical ^{15}N NMR data for Ampullosporin A.

Site	Bond vector	Reference plane	α [°]	β [°]	γ [°]	ϵ_{33} [ppm]	ϵ_{22} [ppm]	ϵ_{11} [ppm]	ϵ^{iso} [ppm]
<i>Trp1</i>	N445 – H121	C344; N445; C298	6.9	16.5	21.0	230.8	87.6	59.8	126.1
<i>Ala2</i>	N440 – H124	C297; N440; C296	14.4	17.2	29.2	240.8	73.5	63.4	125.9
<i>Aib3</i>	N439 – H116	C295; N439; C294	2.9	14.2	11.1	230.1	81.9	70.1	127.4
<i>Aib4</i>	N438 – H115	C293; N438; C292	5.3	16.8	25.6	225.3	78.3	68.3	124.0
<i>Leu5</i>	N437 – H120	C291; N437; C290	1.7	19.3	15.4	220.8	74.1	53.0	116.0
<i>Aib6</i>	N436 – H125	C289; N436; C288	6.0	13.1	26.8	235.4	80.9	66.5	127.6
<i>Gln7</i>	N435 – H123	C287; N435; C286	0.8	19.0	13.3	216.2	77.0	50.2	114.5
<i>Aib8</i>	N434 – H119	C285; N434; C284	6.9	13.7	57.7	232.8	80.5	70.6	128.0
<i>Aib9</i>	N433 – H114	C283; N433; C282	2.5	13.9	25.0	228.4	80.2	66.8	125.1
<i>Aib10</i>	N432 – H127	C281; N432; C280	3.6	14.0	5.5	228.7	86.1	68.8	127.9
<i>Gln11</i>	N431 – H118	C279; N431; C278	6.3	19.8	22.1	215.6	74.3	46.8	112.2
<i>Leu12</i>	N430 – H117	C277; N430; C276	4.1	19.3	48.9	220.6	75.1	54.6	116.7
<i>Aib13</i>	N429 – H130	C275; N429; C274	16.9	13.0	36.8	238.2	79.0	67.8	128.3
<i>Gln14</i>	N428 – H133	C273; N428; C272	1.8	20.4	7.9	212.0	62.8	53.4	109.4
<i>Leu15</i>	N427 – H126	C271; N427; C270	1.1	15.2	1.2	232.3	76.6	65.1	124.6

Table 3. The average PAW-revPBE-vdW-DF theoretical values of the ^{15}N NMR parameters for 7 Aib, 8 classical, and all 15 residues of Ampullosporin A (the available experimental data are shown in parentheses).

Parameter	Aib sites	Non-Aib sites	All
ε_{33} (ppm)	231.3 ± 4.5 (232.5) ^{*1}	223.6 ± 10.0 (220.5) ^{*1}	227.2 ± 8.6
ε_{22} (ppm)	81.0 ± 2.5 (85.5) ^{*1}	75.1 ± 6.7 (73.5) ^{*1}	77.9 ± 5.9
ε_{11} (ppm)	68.4 ± 1.6 (64.5) ^{*1}	55.8 ± 6.4 (52.5) ^{*1}	61.7 ± 8.0
ε^{iso} (ppm)	126.9 ± 1.7 (127) ^{*1}	118.2 ± 6.5 (115) ^{*1}	122.2 ± 6.5
α (degrees)	6.3 ± 4.9	4.6 ± 4.6	5.4 ± 4.7
β (degrees)	14.1 ± 1.3	18.4 ± 1.8	16.4 ± 2.7
γ (degrees)	26.9 ± 17.1	30.9 ± 14.6	29.0 ± 15.7

^{*1} Salnikov *et al.* 2009b.

Also on the basis of the comparison between the PAW-revPBE-vdW-DF results and experiment for the small systems described above, the values of α , β , γ angles obtained for the amidic nitrogen sites throughout the AmpA backbone are supposed to be accurately predicted (Table 2 and the mean values in Table 3). As expected (Wadell *et al.* 2005), the angle α , which represents the tilt off the peptide plane of the most shielded direction of the ^{15}N CST, was found to be very small. Specifically, only for two residues (Aib3 and Ala12) its value exceeds 10° , and there is no apparent trend in its variation. The values of the angle β (between the $\text{N}_{\text{amid}} - \text{H}_{\text{amid}}$ bond and the most shielded direction of the ^{15}N CST) were calculated to lie in the interval from 13 to 20 degrees. They are thus consistent with the results for proteins, which were established from the solution NMR relaxation studies (Fushman *et al.* 1998) and from the NMR residual shielding measurements (Cornilescu *et al.* 2000). It should be noted that these values are of importance in the NMR cross-correlation investigations of proteins (Kadeřávek *et al.* 2015). The β angles of Aib residues, with the average value of 14° , are generally smaller than those for classical amino acids (averaging

18°). However, a bigger data set of peptaibols would be needed to confirm if this is a systematic trend, as even in AmpA the β angle at Aib4 is larger than the one found at Leu15 (Table 2). Interestingly, there is a considerable variation in the angle γ (describing the departure of the mid-shielded direction of the ^{15}N CST from orthogonality to the peptide plane), with its values ranging from close to zero to more than 50° in the case of Aib8. There are no longer fragments of AmpA with either lower or higher γ values, and the standard deviation of the averages is high for both Aib and the remaining sites (Tables 2 and 3). This and other completely site-specific effects are not taken into account in an analysis of the $\text{N}_{\text{amid}} - \text{H}_{\text{amid}}$ dipolar and N_{amid} chemical shift anisotropy cross-correlated relaxation rates (Palmer 2004).

Conflict of Interest

There is no conflict of interest.

Acknowledgements

The work was supported by the Ministry of Education, Youth and Sports of CR within the National Sustainability Program I, Project LO1507 POLYMAT.

References

- BECHINGER B: The SMART model: soft membranes adapt and respond, also transiently, in the presence of antimicrobial peptides. *J Pept Sci* **21**: 346-355, 2015.
- BLOCHL PE: Projector augmented-wave method. *Phys Rev B* **50**: 17953-17979, 1994.
- BONHOMME C, GERVAIS C, BABONNEAU F, COELHO C, POURPOINT F, AZAIS T, ASHBROOK SE, GRIFFIN JM, YATES JR, MAURI F, PICKARD CJ: First-principles calculation of NMR parameters using the gauge including projector augmented wave method: a chemist's point of view. *Chem Rev* **112**: 5733-5779, 2012.
- CHARPENTIER T: The PAW/GIPAW approach for computing NMR parameters: a new dimension added to NMR study of solids. *Solid State Nucl Magn Reson* **40**: 1-20, 2011.

- CORNILESCU G, BAX A: Measurement of proton, nitrogen and carbonyl chemical shielding anisotropies in a protein dissolved in a dilute liquid crystalline phase. *J Am Chem Soc* **122**: 10143-10154, 2000.
- CZERNEK J, BRUS J: Theoretical predictions of the two-dimensional solid-state NMR spectra: a case study of the $^{13}\text{C} - ^1\text{H}$ correlations in metergoline. *Chem Phys Lett* **586**: 56-60, 2013.
- CZERNEK J, PAWLAK T, POTRZEBOWSKI MJ, BRUS J: The comparison of approaches to the solid-state NMR-based structural refinement of vitamin B-1 hydrochloride and of its monohydrate. *Chem Phys Lett* **555**: 135-140, 2013.
- CZERNEK J, BRUS J: The covariance of the differences between experimental and theoretical chemical shifts as an aid for assigning two-dimensional heteronuclear correlation solid-state NMR spectra. *Chem Phys Lett* **608**: 334-339, 2014.
- CZERNEK J: On the solid-state NMR spectra of naproxen. *Chem Phys Lett* **619**: 230-235, 2015.
- DAL CORSO A: Pseudopotentials periodic table: From H to Pu. *Comput Mater Sci* **95**: 337-350, 2014.
- DU L, RISINGER AL, MITCHELL CA, YOU J, STAMPS BW, PAN N, KING JB, BOPASSA JC, JUDGE SIV, YANG Z, STEVENSON BS, CICHEWICZ RH: Unique amalgamation of primary and secondary structural elements transform peptaibols into potent bioactive cell-penetrating peptides. *Proc Natl Acad Sci U S A* **114**: 8957-8966, 2017.
- FUSHMAN D, TJANDRA D, COWBURN D: Direct measurement of ^{15}N chemical shift anisotropy in solution. *J Am Chem Soc* **120**: 10947-10952, 1998.
- GIANOZZI P, BARONI S, BONINI N, CALANDRA M, CAR R, CAVAZZONI C, CERESOLI D, CHIAROTTI GL, COCCIONI M, DABO I, DAL CORSO A, DE GIRONCOLI S, FABRIS S, FRATESI G, GEBAUER R, GERSTMANN U, GOUGOUSSIS C, KOKALJ A, LAZZEN M, MARTIN-SAMOS L, MARZANI N, MAURI F, MAZZARELLO R, PAOLINI S, PASQUARELLO A, PAULATTO L, SBRACCIA C, SCANDOLO S, SCLAUZERO G, SEITSONEN AP, SMOGUNOV A, UMARI P, WENTZCOVITCH RM: QUANTUM ESPRESSO: a modular and open-source software project for quantum simulations of materials. *J Phys Condens Matter* **21**: 395502, 2009.
- HARMOUCHE N, AISENBREY C, PORCELLI F, XIA Y, NELSON SED, CHEN X, RAYA J, VERMEER L, APARICIO C, VEGLIA G, GORR SU, BECHINGER B: Solution and solid state nuclear magnetic resonance structural investigations of the antimicrobial designer peptide GL13K in membranes. *Biochemistry* **56**: 4269-4278, 2017.
- HARRIS RK, HODGKINSON P, PICKARD CJ, YATES JR, ZORIN V: Chemical shift computations on a crystallographic basis: some reflections and comments. *Magn Reson Chem* **45**: S174-S186, 2007.
- KADEŘÁVEK P, GRUTSCH S, SALVI N, TOLLINGER M, ŽÍDEK L, BODENHAUSEN G, FERRAGE F: Cross-correlated relaxation measurements under adiabatic sweeps: determination of local order in proteins. *J Biomol NMR* **63**: 353-365, 2015.
- KALAKEWICH K, IULIUCCI R, MUELLER KT, ELORANTA H, HARPER JK: Monitoring the refinement of crystal structures with N-15 solid-state NMR shift tensor data. *J Chem Phys* **143**: 194702, 2015.
- KRONEN M, GÖRLS H, NGUYEN HH, REISSMANN S, BOHL M, SÜHNEL J, GRÄFE U: Crystal structure and conformational analysis of Ampullosporin A. *J Pept Sci* **9**: 729-744, 2003.
- MOLUGU TR, LEE S, BROWN MF: Concepts and methods of solid-state NMR spectroscopy applied to biomembranes. *Chem Rev* **117**: 12087-12132, 2017.
- MONKHORST HJ, PACK JD: Special points for Brillouin-zone integrations. *Phys Rev B* **13**: 5188-5192, 1976.
- NAGAO T, MISHIMA D, JAVKHLANTUNGS N, WANG J, ISHIOKA D, YOKOTA K, NORISATA K, KAWAMURA I, UEDA K, NAITO A: Structure and orientation of antibiotic peptide alamethicin in phospholipid bilayers as revealed by chemical shift oscillation analysis of solid state nuclear magnetic resonance and molecular dynamics simulation. *Biochim Biophys Acta* **1848**: 2789-2798, 2015.
- PALMER AG: NMR characterization of the dynamics of biomacromolecules. *Chem Rev* **104**: 3623-3640, 2004.
- RITZAU M, HEINZE S, DORNBERGER K, BERG A, FLECK W, SCHLEGEL B, HÄRTL A, GRÄFE U: Ampullosporin, a new peptaibol-type antibiotic from *Sepedonium ampullosporum* HKI-0053 with neuroleptic activity in mice. *J Antibiot (Tokyo)* **50**: 722-728, 1997.

-
- SABATINI R, KÜÇÜKBENLİ E, KOLB B, THONHAUSER T, DE GIRONCOLI S: Structural evolution of amino acid crystals under stress from a non-empirical density functional. *J Phys Condens Matter* **24**: 424209, 2012.
- SALNIKOV ES, FRIEDRICH H, LI X, BERTAIN P, REISSMANN S, HERTWECK C, ONEIL JDJ, RAAP J, BECHINGER B: Structure and alignment of membrane-associated peptaibols Ampullosporin A and Alamethicin by oriented ^{15}N and ^{31}P solid-state NMR spectroscopy. *Biophys J* **96**: 86-100, 2009.
- SALNIKOV E, BERTANI P, RAAP J, BECHINGER B: Analysis of the amide ^{15}N chemical shift tensor of the C_α tetrasubstituted constituent of membrane-active peptaibols, the α -aminoisobutyric acid residue, compared to those of di- and tri-substituted proteinogenic amino acid residues. *J Biomol NMR* **45**: 373-387, 2009.
- SOSS SE, FLYNN PF, IULIUCCI RJ, YOUNG RP, MUELLER RJ, HARTMAN J, BERAN GJO, HARPER JK: Measuring and modeling highly accurate N-15 chemical shift tensors in a peptide. *Chemphyschem* **18**: 2225-2232, 2017.
- WADELL KW, CHEKMENEV EY, WITTEBORT RJ: Single-crystal studies of peptide prolyl and glycyl ^{15}N shielding tensors. *J Am Chem Soc* **127**: 9030-9035, 2005.
- WU CH, RAMAMOORTHY A, OPELLA SJ: High-resolution heteronuclear dipolar solid-state NMR spectroscopy. *J Magn Reson A* **109**: 270-272, 1994.
-